INSTITUTE FOR FUSION STUDIES

DE-FG03-96ER-54346-784 IFSR #784

Studies of Instability and Transport in Tokamak Plasmas with Very Weak Magnetic Shear

J.Q. DONG, Y.Z. ZHANG
Southwestern Institute of Physics, Chengdu, P.R. China
& International Center for Theoretical Physics, Trieste, Italy
and
S.M. MAHAJAN
Institute for Fusion Studies
The University of Texas at Austin
Austin, Texas 78712 USA

April 1997

THE UNIVERSITY OF TEXAS

AUSTIN

HH

Studies of instability and transport in tokamak plasmas with very weak magnetic shear

J.Q. Dong, Y.Z. Zhang

Southwestern Institute of Physics, Chengdu, P.R. China

and International Center for Theoretical Physics, Trieste, Italy

and S.M. Mahajan

Institute for Fusion Studies, The University of Texas at Austin, Austin, USA

(April 29, 1997)

Abstract

Ion temperature gradient (ITG or η_i) driven microinstabilities are studied, using kinetic theory, for tokamak plasmas with very weak (positive or negative) magnetic shear (VWS). The gradient of magnetic shear as well as the effects of parallel and perpendicular velocity shear ($v'_{\|}$ and v'_E) are included in the defining equations. Two eigenmodes: the double (D) and the global (G) are found to coexist. Parametric dependence of these instabilities, and of the corresponding quasilinear transport is systematically analyzed. It is shown that, in VWS plasmas, a parallel velocity shear (PVS) may stabilize or destabilize the modes, depending on the individual as well as the relative signs of PVS and of the gradient of magnetic shear. The quasilinear transport induced by the instabilities may be significantly reduced with PVS in VWS plasmas. The v'_E values required to completely suppress the instabilities are much lower in VWS plasmas than they are in normal plasmas. Possible correlations with tokamak experiments are discussed.

52.55.Fa, 52.35.Kt, 52.35.Ra

I. INTRODUCTION

One of the major goals of recent tokamak experiments has been to investigate and determine optimal operational conditions which will lead to long-lived discharges with enhanced confinement and reactor-like plasma parameters. A particularly promising regime was uncovered recently by a manipulation of the current density profile to create a negative (reversed) magnetic shear region in the main body of the plasma. On many devices,[1–3] dramatic particle and energy confinement improvements are observed in these regions. It is natural that an explanation of these experimental results should be sought in the effects such optimized magnetic configurations have on microinstabilities, and on the consequent turbulent transport. This provided the main motivation for a recent paper[4] in which two important instabilities of a standard plasma (with positive magnetic shear), the ITG (ion temperature gradient), and the PVS (parallel velocity shear) modes were studied for plasmas with negative magnetic shear. From an integral gyrokinetic analysis, it was found that in toroidal geometry, the conventional modes not only have lower growth rates, but also have higher instability thresholds when the sign of the magnetic shear is reversed.

Theoretical estimates, however, reveal that the lowering of the virulence of the instabilities caused by negative magnetic shear is perhaps not sufficient to account for the experimentally observed spectacular improvement in confinement. Therefore, more experimental and theoretical studies are needed to delineate the related physics.

One notable characteristic of the optimized configuration is that, besides the negative magnetic shear at small radii, there is positive but weak magnetic shear at intermediate radii.[1,5] In other words, a relatively broad transition region exists where the magnetic shear, positive or negative, is very weak (even close to zero). It is also clearly evident from the experimental data[1,5] that the region of improved confinement is not limited to the radial region with reversed shear but it extends deep into the region of reduced but positive shear.

DISCLAIMER

Within the general category of negative central magnetic shear (NCS) experiments on DIII-D,[5] a new subclass of discharges with a broad region of weak or slightly negative magnetic shear (WNS), have also been investigated. This subclass is comparable to the standard NCS discharges in good confinement, high fusion reactivity, and a large fraction of bootstrap current, but shows higher β values. In fact, the DIII-D experiments reached their highest normalized β, and confinement enhancement in the WNS configuration.

In the WNS(VWS) magnetic geometry, there is a finite transition region (where the shear changes sign) of near zero shear. It is important to notice that the best confinement is measured precisely in the neighborhood of this unusual region.[1,5] Since most of the existing instability theories were derived for finite shear, it is clear that a new (certainly a modified one) microinstability theory must be developed to deal with this important and interesting region. Only then, one might be able to establish a possible connection between improved confinement and mode-stabilization in the new shear geometry.

Before deriving the new equations, we must dwell on another crucial experimental observation,[3,5,6] the existence of a strongly peaked ion toroidal velocity (with a larger PVS) in the region of improved confinement. It is also known[7,8] that a large PVS may play an important role in the improved particle confinement of ions, and that the PVS induced asymmetric Reynolds stress may be a possible source for the perpendicular (or $\mathbf{E} \times \mathbf{B}$) velocity shear generation. Thus an explanation of improved confinement in VWS plasmas is likely to require an understanding of the effects of PVS on the mode-stability in a plasma with very low magnetic shear.

In this work, we study the drift-type microinstabilities driven by ITG and PVS in kinetic plasmas with VWS structures. In Sec. II, we explain the physical model, and display the modified eigenmode equation in a sheared slab. The gradient of magnetic shear (an essential factor in this regime), the interaction between ITG and PVS, and the suppression effects of the $\mathbf{E} \times \mathbf{B}$ perpendicular velocity shear are all taken into account. The numerical results

on the eigenvalues and the mode structure for various parameters are presented in Sec. III. An estimate for the quasilinear transport induced by the fluctuations is also calculated and displayed. In Sec. IV, we recapitulate the main conclusions of this work and discuss their implications.

II. PHYSICAL MODEL AND EIGENMODE EQUATION

In a slab model, the principal modification to the standard kinetic theory, so that it can adequately deal with the low shear regime, is to write the equilibrium magnetic field as

$$\mathbf{B} = B_0[\hat{\mathbf{z}} + (x/L_s + x^2/L_{s2})\hat{\mathbf{y}}], \tag{1}$$

where L_s, and $L_{s2} = (d/dx)(1/L_s)$ are the measures of the magnetic shear and its gradient. The x, y, and z directions in the sheared slab geometry mimic the radial, poloidal, and toroidal directions in a tokamak. The modes are usually confined in the vicinity of the rational surface defined by $k_{\|} = \mathbf{k} \cdot \mathbf{B} = 0$, where $\mathbf{k}$ is the wave vector for the perturbation, and $\mathbf{B}$ is the total magnetic field given in Eq. (1). The third term on the right-hand side of Eq. (1) is important only when the magnetic shear is very weak ($L_s \to \infty$) at the mode rational surface ($x = 0$).

The kinetic differential dispersion equation for the above magnetic configuration is easy to obtain.[9,10] In order to concentrate on the new physics peculiar to this geometry, it is essential to use a reasonably simplified model: we treat only the ion dynamics in detail; the electron response is taken to be adiabatic. Both PVS and perpendicular velocity shear of ions are assumed to be spatially independent. In the long wavelength approximation, $k\rho_i \ll 1$ (ρ_i is the ion Larmor radius), the normalized perturbed electrostatic potential $\phi(x)$ obeys

$$\frac{d^2\phi(x)}{dx^2} - b_s\phi(x) + \frac{P(x)}{R(x)}\phi(x) = 0, \tag{2}$$

where

$$P(x) = 1 + \tau(1 + \zeta_i Z(\zeta_i)) + \frac{\omega_{*e}}{|k_\parallel| v_{ti}} \left\{ Z(\zeta_i) + \eta_i \left[\zeta_i + \left(\zeta_i^2 - \frac{1}{2} \right) Z(\zeta_i) \right] \right\} - 2v'_\parallel \frac{\omega_{*e}}{k_\parallel v_{ti}} (1 + \zeta_i Z(\zeta_i)), \tag{3}$$

$$R(x) = \zeta_i Z(\zeta_i) + \frac{\omega_{*e}}{|k_\parallel| v_{ti}} \left\{ Z(\zeta_i) \eta_i \left[\zeta_i + \left(\zeta_i^2 + \frac{1}{2} \right) Z(\zeta_i) \right] \right\} - 2v'_\parallel \frac{\omega_{*e}}{k_\parallel v_{ti}} (1 + \zeta_i Z(\zeta_i)), \tag{4}$$

and $\phi(x, y, t) = \phi(x) \exp(ik_y y - i\omega t)$. The notation is standard: $\tau = T_e/T_i$ is the ratio of the electron to the ion temperature, $v'_\parallel = (L_n/c_s)(dv_\parallel/dx)$ is the normalized PVS, $\eta_i = L_n/L_{Ti}$ is ion temperature gradient parameter, ω_{*e} is electron diamagnetic drift frequency, L_n is the density scale length, $b_s = k_y^2 \rho_s^2$, $c_s = \sqrt{T_e/m_i}$ is the speed of sound, v_{ti} is ion thermal velocity, and $\rho_s = c_s/\Omega_i$ with Ω_i being the ion gyrofrequency in the toroidal magnetic field.

The main change brought about by the new expression for the magnetic field (needed to describe the VWS system) in the mode equation can be seen in the argument of the plasma dispersion function $Z(\zeta_i)$,

$$\zeta_i = \frac{\omega - k_\parallel v_\parallel - k_y v_E}{|k_\parallel| v_{ti}} = \sqrt{\frac{\tau}{2}} \frac{\hat{\omega} - x v'_E}{|x(s + s_2 x)|}, \tag{5}$$

which now contains the parameter s_2 absent in the conventional formulation. In Eq. (5),

$$\hat{\omega} = \frac{\omega}{\omega_{*e}}, \quad s = \frac{L_n}{L_s}, \quad s_2 = \frac{L_n \rho_s}{L_{s2}}, \quad v'_E = \frac{L_n}{c_s} \frac{dv_E}{dx},$$

and x is normalized to ρ_s.

It is easy to notice that when velocity shear effects are neglected, the eigenvalue of Eq. (2) is independent of the signs of s and s_2. The eigenfunction, however, is shifted to right (left) with respect to the mode rational surface when the signs are opposite (same). The s_2 term is important only in the region (in the vicinity of mode rational surface where the eigenmode is confined) where $x \gtrsim s/s_2$. Generally speaking, the typical mode-width is determined by ion Landau damping scale defined by $\omega \sim k_\parallel v_{ti}$ which gives $x \sim \sqrt{\tau}\hat{\omega}/\sqrt{2}s$ when s_2 is neglected. Thus, a necessary condition for the s_2 term to significantly influence the mode is

$$s_2 \gtrsim \frac{\sqrt{2}s^2}{\sqrt{\tau}\widehat{\omega}}. \tag{6}$$

From Eq. (5), it is straightforward to see that an additional resonant surface, besides the rational surface at $x = 0$, appears at $x = -s/s_2$ if condition Eq. (6) holds. This is expected to bring more free energy for destabilization in a particular parameter regime. The most significant effects introduced by the gradient of the magnetic shear in VWS plasmas are the changes in the mode structure and the consequent effects on driving or damping.

III. NUMERICAL RESULTS

In this section, we present the salient aspects of the results obtained by solving Eq. (2) using a WKB shooting code. Unless stated otherwise, the following parameters : $\tau = 1, \eta_i = 3, s_2 = -0.01, b_s = 0.1$, will be kept fixed while the others (like s) are varied. For a given set of parameters, two distinct modes with significantly different structures emerge; this is similar to what was found for the tearing modes in a parabolic q-profile.[11] Typical eigenfunctions are given in Fig. 1 where the real parts of the perturbed potential ϕ_r are plotted versus the radial coordinate x for several values of s, the magnetic shear parameter. For the modes displayed in Fig. 1(a), ϕ_r has two well-defined peaks whose separation increases rapidly with increasing magnetic shear. As expected, these peaks appear at the two resonant surfaces, $x = 0$ and $x = -s/s_2$. Hereafter, this mode will be referred to as the double (D) mode. In contrast, the plots in Fig. 1(b) have a more global structure and correspond to what will be called the global (G) mode. In the latter case, the coupling between the two resonances is rather strong leading to a two-peak structure (of ϕ_r) not quite as pronounced as it is for the D-mode. When the magnetic shear s is negligibly small, both of these modes are centered at the mode rational surface since the two resonant surfaces are close to each other. The additional resonant surface is pushed away from the rational surface when the magnetic shear increases. For the D-mode, the coupling between the two resonances decreases rather

rapidly and finally vanishes with increasing magnetic shear; at this stage the mode is still unstable. On the other hand, with increasing shear, the coupling between the two resonances of the G-mode decreases slowly and becomes negligible only when the mode becomes stable.

A. Instability and transport—no velocity shear

In this subsection, the interesting but complicating effects of velocity shear are neglected. The normalized growth rate (a) and real part of the frequency (b) are shown in Fig. 2 as functions of s for both the D- and the G-mode. For both kinds of modes, the growth rate increases in the VWS region ($s \leq 0.1$, here), and then decreases with increasing magnetic shear. The growth rate of the D-mode is lower than that of the G-mode in the VWS regime. However, in the parameter regime studied here, the G-mode is stabilized at $s \sim 0.22$. At this value of s, the D-mode is still noticeably unstable. The mode structures shown in Fig. 1 hold the secret for this difference: the eigenfunction for the G-mode becomes broader with increasing magnetic shear, and the stabilization results due to enhanced Landau damping. At comparable shear, the two resonances comprising the D-mode decouple from each other and the mode behavior will effectively correspond to that of a singly peaked mode; the mode shrinks in size and hence suffers less ion Landau damping.

The real frequency of the G-mode is much higher than that of the D-mode. Both modes rotates in the ion direction and their respective frequencies increase with increasing magnetic shear. For zero s, the real frequency of the D-mode goes to zero and it is $\sim 0.5\omega_{*e}$ for the G-mode.

In Fig. 3, the normalized growth rate and the real frequency (for both D- and G-mode) are plotted as functions of s_2, the parameter measuring the gradient of the magnetic shear $\hat{s}$. For G-mode, the growth rate increases slightly first, and then decreases very rapidly as s_2 increases; the mode is stabilized at $s_2 \sim 0.02$. This holds for both of the displayed $s = 0.001$

and $s = 0.11$ cases. In contrast, for the D-mode, the results for $s = 0.0001$ and $s = 0.1$ are qualitatively different for $s_2 \lesssim 0.03$; the effects of magnetic shear are quite negligible for $s_2 \gtrsim 0.1$. In the low s_2 region, the growth rate of the D-mode increases (decreases) for $s = 0.1$ ($s = 0.0001$) as s_2 decreases. At $s \sim 0.1$, the D-mode survives only if s_2 approaches zero. It may be safely concluded, therefore, that the D-mode is the VWS version of the conventional ITG mode, and that the gradient of magnetic shear has a stabilizing effect on it.

The real frequencies for both the modes increase with s_2 with the G-modes increasing much faster than the D-modes. The real frequency of the D-mode is always much lower than the electron diamagnetic frequency ω_{*e}, while for the G-mode it is comparable with ω_{*e}.

The mixing length estimates for the transport, $\gamma * \Delta^2$, induced by these modes are shown in Fig. 4 as functions of s. Here, γ is the normalized growth rate, and Δ is the averaged mode width normalized to ρ_s. The averaged mode width as well as the displacement of the mode center from the rational surface can be readily defined as the weighted averages

$$x_0 = \frac{\int x|\phi(x)|^2 dx}{\int |\phi(x)|^2 dx}, \tag{7}$$

and

$$\Delta^2 = \frac{\int (x - x_0)^2 |\phi(x)|^2 dx}{\int |\phi(x)|^2 dx}. \tag{8}$$

It is clear from Fig. 4 that if D-mode were dominant, the transport would considerably decrease for low magnetic shear. The transport due to G-mode, however, does not change much with magnetic shear. Compared to D-mode, the G-mode induced transport is higher in the VWS region and lower in the moderate shear region.

Thus, from the results shown in Fig. 4, a possible scenario for improved confinement in the VWS plasmas emerges: if the parameter s_2 is high enough so that the G-mode is stabilized,

the total transport will precipitously fall because the D-mode contribution is rather small. This is eminently possible since the values required are not very high (see Fig. 3(a)).

If this mechanism turns out to be inadequate (for example if s_2 is not high enough) additional physical elements such as velocity shear will have to be introduced in the theory in order to explain experimental observations.

B. Parallel velocity shear effects

We begin by introducing the effects of a PVS on the instabilities just discussed. In Fig. 5, we show how the mode growth rate (a), and the real frequency (b) change with PVS. An examination of the relevant terms in Eq. (2) reveal that the eigenvalue is independent of the sign of the PVS when the s_2 term is not included. With the inclusion of the gradient of magnetic shear, the symmetry with respect to the $v'_{\parallel} = 0$ axis is broken as shown in Fig. 5. In the VWS region (the curves for $s = 0.005$ and $s = 0.001$), a negative PVS has a strong stabilizing influence on both the G- and the D-mode and a positive PVS is destabilizing for $s_2 < 0$ and $s > 0$. For larger s ($s = 0.15$, for example), a negative PVS is alway destabilizing for both modes. A positive PVS is stabilizing for the G-mode, but for the D-mode, it is slightly stabilizing for low values, and becomes destabilizing for larger values.

It is well known that a PVS enhances the ITG driving mechanism and that this effect is independent of the sign of the PVS in plasmas with not very low magnetic shear.[10,12] Our results for the D-mode at $s = 0.15$ (moderate shear) are in complete agreement with this conclusion. However, as shown above, our results for VWS plasmas are completely different from these standard results. An obvious implication is that most of the microinstability theories valid for magnetically confined plasmas with moderate or strong shear will need to be seriously reexamined, and possibly modified, to extend their validity to VWS plasmas.

The modes rotate in ion direction except that the D-mode turns to rotate in electron

direction for some parameters; for example, $s = 0.005$ and $v'_{\|} \geq 0.3$. For both modes, the effects of a PVS on the real frequency in VWS plasmas are opposite to that found in the normal ones. As it increases from -1 to 1, a PVS pushes the modes to the ion diamagnetic direction at $s = 0.15$, and to the electron direction at $s = 0.005$ ($s = 0.001$) for the D-mode (G-mode).

It is worthwhile to point out that the results for $s_2 = 0.01$ are the mirror image (with respect to the $v'_{\|} = 0$ axis) of Fig. 5. This can be seen from the dispersion equation (2).

The quasilinear mixing length estimate of the transport is plotted versus PVS in Fig. 6. The transport induced by the D-mode is much lower in the $s = 0.005$ VWS plasmas than it is in the moderately sheared plasma with $s = 0.15$ for the broad range of PVS from -1 to 1. A positive PVS enhances the D-mode induced transport for both low $s = 0.005$ and moderate $s = 0.15$. In contrast, a negative PVS reduces the transport for low $s = 0.005$, and increases it slightly for the moderate $s = 0.15$. The situation for the G-mode related transport is similar. For $s = 0.001$, it is one order of magnitude lower at $v'_{\|} = -1$ than it is at $v'_{\|} = 0$, and is close to that induced by the D-mode. At $s = 0.15$, the G-mode induced transport is lower (higher) than it is for $s = 0.001$ when $v'_{\|} > 0$ ($v'_{\|} < 0$). In conclusion, a PVS may bring down the turbulent G-mode induced transport by a factor of 10 from the value without PVS effects in VWS plasmas. Thus, the total transport in VWS plasmas ($s \sim 0.001$) is significantly lower than it is in plasmas with moderate magnetic shear ($s \sim 0.1$). This is certainly in line with the experimental observations.[3,5,6]

C. Perpendicular velocity shear effects

The effects of a perpendicular velocity shear v'_E on G-mode are given in Fig. 7 where the normalized growth rate (a) and the real frequency (b) are shown as function of v'_E. The stabilization effects of v'_E are clearly evident. The v'_E values required to completely suppress

the instabilities are much lower at low shear ($s = 0.001$) than they are at moderate shear ($s = 0.15$) for $v'_{\|}$ ranging from -1 to 0. The most noticeable difference occurs at $v'_{\|} = -1$ where at $s = 0.15$, stability is achieved at $v'_E \leq -0.2$ or $v'_E \geq 0.15$ while much smaller $|v'_E| \geq 0.02$ is required for mode stabilization when $s = 0.001$. For $v'_{\|} = 1$, on the other hand, the required v'_E to completely suppress the mode is higher at $s = 0.001$ than it is at $s = 0.15$. However, the difference is not significant. Considering that the growth rate for the former is about five times higher than that for the latter, it is legitimate to conclude that the suppression effect of perpendicular velocity shear is stronger in VWS than it is in a plasma with high or moderate magnetic shear. This is qualitatively in line with the finding from the investigation with a toroidal integral kinetic equation, that suppression effect of a perpendicular velocity shear on the instabilities is stronger in regions with low magnetic shear than it is in plasmas with high shear.[12]

The mode rotates in the ion direction except for $s = 0.15$ and $v'_{\|} = 0$ or -1 for which the mode turns to rotate in electron direction with $\omega \sim \omega_{*e}$ when $v'_E \sim 0.1$.

In Fig. 8, the eigenfrequency of the D-mode is displayed. The legend for Fig. 8 is the same as that of Fig. 7 except that in Fig. 8, $s = 0.005$ instead of $s = 0.001$. Again, the required v'_E to completely suppress the mode is lower at $s = 0.005$ (the open symbols) than it is at $s = 0.15$ (the close symbols) for $v'_{\|}$ values from -1 to 0. Even for $v'_{\|} = 1$, the window in which the mode is unstable is wider ($-0.34 \leq v'_E \leq 0.18$) at $s = 0.15$ than it is ($-0.26 \leq v'_E \leq 0.26$) at $s = 0.005$.

The dependence of the real frequency on v'_E for the D-mode is quite different from that of the G-mode. Now, the mode rotates in the electron direction at $s = 0.005$ if $0 \leq v'_{\|} \leq 1$ and $0.05 \leq |v'_E|$. For $s = 0.15$, the D-mode rotates in the electron direction with $\omega \sim \omega_{*e}$ only for $v'_{\|} = -1$ when $v'_E > 0$. This is in contrast to that for the G-mode where the mode rotates in electron direction for both $v'_{\|} = -1$ and 0 when $v'_E > 0$ and $s = 0.15$.

IV. CONCLUSIONS AND DISCUSSION

Using kinetic ion and adiabatic electron responses, we have investigated drift-type microinstabilities driven by ion temperature gradient (ITG or η_i) in tokamak plasmas embedded in very weakly sheared magnetic fields (VWS). In this regime, the gradient of magnetic shear plays an essential role in determining the stability as well as the structure of the eigenmode. We have also included the effects of parallel and perpendicular velocity shear and studied the interplay of these two 'shears'. Numerical solutions reveal the simultaneous presence of two distinct structures respectively called the double (D) and the global (G) mode. Parametric dependence of these instabilities and of the corresponding induced quasilinear transport is systematically analyzed.

It is found that the modes are less unstable in VWS plasmas than they are in plasmas with moderate or strong magnetic shear. It is also shown, however, that the instability properties and the confinement in VWS plasmas do not differ significantly from those in normal ones when PVS and perpendicular velocity shear effects are not included and the parameter s_2 for the gradient of magnetic shear is not high enough to suppress G-mode.

Inclusion of PVS in VWS plasmas is found to stabilize or destabilize the modes, depending on its intrinsic sign and also on its sign relative to the gradient of the magnetic shear. This is in distinct contrast with the behavior of a standard (moderate to strong shear) plasma which is always destabilized by PVS.[10,12] In addition, the quasilinear mixing length transport induced by these modes is estimated to be significantly (more than one order of magnitude) reduced by a negative PVS for $s_2 = -0.01$ in VWS plasmas compared to the values in normal plasmas. A positive PVS is expected to have the same effects for positive $s_2 = 0.01$.

The perpendicular velocity shear has equally strong effect on the instabilities in VWS plasmas. It is found that v'_E values required to completely suppress the instability are much lower at $s \sim 0.001$ than they are at $s \sim 0.1$ for $v'_\parallel \leq 0$ (≥ 0) when the gradient of magnetic

shear is negative (positive).

The experimental results [3,5,6] have shown a strong peaking of plasma toroidal rotation frequency Ω_ϕ in the region of improved confinement. The preceding simple theoretical model seems to suggest a possible basis for the correlation between improved confinement and PVS. It is proposed that a strong stabilization of the microinstabilities brought about by a combination of very weak shear and a large PVS might lie at the heart of significantly improved ion confinement. It is also likely that the gradient of PVS-induced Reynolds stress may be the driving force for the perpendicular (or $\mathbf{E} \times \mathbf{B}$) velocity shear which further suppresses turbulence and the corresponding transport.[7,8]

In order to focus on the basic physical processes, the toroidal and finite Larmor radius effects are neglected in this paper. These are expected to be important in high temperature tokamak plasmas. Studies on these effects are in progress and will be published separately.

Acknowledgment

One of the authors (J.Q.D.) would like to thank the International Center for Theoretical Physics, Trieste Italy for hospitality.

Work supported by National Natural Science Foundation of China, by International Center for Theoretical Physics, and by U.S. Dept. of Energy contract #DE-FG03-96ER-54346.

REFERENCES

[1] M. Hugon, B.Ph. van Milligen, P. Smeulders, L.C. Appel, D.V. Bartlett, D. Doucher, A.W. Edwards, L.-G. Eriksson, C.W. Gowers, T.C. Hender, G. Huysmans, J.J. Jacquinot, P. Kupschus, L. Porte, P.H. Rebut, D.F.H. Start, F. Tibone, B.J.D. Tubbing, M.L. Watkins, W. Zwingmann, Nucl. Fusion **32**, 33 (1992).

[2] F.M. Levinton, M.C. Zarnstorff, S.H. Batha, M. Bell, R.V. Budny, C. Bush, Z. Chang, E. Fredrickson, A. Janos, J. Manickam, A. Ramsey, S.A. Sabbagh, G.L. Schmidt, E.J. Synakowski, and G. Taylor, Phys. Rev. Lett. **75**, 4417 (1995).

[3] E.J. Strait, L.L. Lao, M.E. Mauel, B.W. Rice, T.S. Taylor, K.H. Burrell, M.S. Chu, E.A. Lazarus, T.H. Osborne, S.J. Thompson, and A.D. Turnbull, Phys. Rev. Lett. **75**, 4421 (1995).

[4] J.Q. Dong, Y.Z. Zhang, S.M. Mahajan, and P.N. Guzdar, Phys. Plasmas **3**, 3065 (1996).

[5] L.L. Lao, K.H. Burrell, T.S. Casper, V.S. Chan, M.S. Chun, J.C. DeBoo, E.J. Doyle, R.D. Durst, C.B. Forest, C.M. Greenfield, R.J. Groebner, F.L. Hinton, Y. Kawano, E.A. Lazarus, Y. R. Lin-Liu, M. E. Mayel, W.H. Meyer, R.L. Miller, G.A. Navratil, T.H. Osborne, Q. Peng, C.L. Rettig, G. Rewoldt, T.L. Phodes, B.W. Rice, D.P. Schissel, B.W. Stallard, E.J. Strait, W.M. Tang, T.S. Taylor, A.D. Turnbull, R.E. Waltz, and the DIII-D Team, Phys. Plasmas **3**, 1951 (1996).

[6] Y. Koide, M. Kikuchi, M. Mori, S. Tsuji, S. Ishida, N. Asakura, Y. Kamada, T. Nishitani, Y. Kawano, T. Hatae, T. Fujita, T. Fukuda, A. Sakasai, T. Kondoh, and Y. Neyatani, Phys. Rev. Lett. **72**, 3662 (1994).

[7] J.Q. Dong, W. Horton, R.D. Bengtson, and G.X. Li, Phys. Plasmas **1**, 3250 (1994).

[8] X.Y. Fu, J.Q. Dong, W. Horton, C.T. Ying, and G.J. Liu, Phys. Plasmas **4**, 588 (1997).

[9] P.J. Catto, M.N. Rosenbluth, and C.S. Liu, Phys. Fluids **16**, 1719 (1973).

[10] M. Artun and W.M. Tang, Phys. Fluids B **4**, 1102 (1992).

[11] S.M. Mahajan, R.D. Hazeltine, Nucl. Fusion **9**, 1191 (1982).

[12] J.Q. Dong and W. Horton, Phys. Fluids B **5**, 1581 (1993).

FIGURE CAPTIONS

FIG. 1. Fig. 1(a) The real part of the eigenfunction for the double (D) mode. The other parameters are $b_s = 0.1,\ \eta_i = 3,\ s_2 = -0.01, \tau = 1,\ v'_{\|} = v'_E = 0$.

(b) The real part of the eigenfunction for the global (G) mode. The other parameters are the same as in Fig. 1(a).

FIG. 2. Normalized growth rate (a) and real frequency (b) versus magnetic shear s for double (D) and global (G) mode. The other parameters are the same as in Fig. 1.

FIG. 3. Normalized growth rate (a) and real frequency (b) versus s_2, the gradient of magnetic shear s, for double (D) and global (G) mode. The other parameters are the same as in Fig. 1.

FIG. 4. Quasilinear turbulent transport versus magnetic shear s for double (D) and global (G) mode. The other parameters are the same as in Fig. 1.

FIG. 5. Normalized growth rate (a) and real frequency versus normalized parallel velocity shear $v'_{\|}$ for global (G) and double (D) mode. The other parameters are the same as in Fig. 1.

FIG. 6. Quasilinear turbulent transport versus normalized parallel velocity shear $v'_{\|}$ for global (G) and double (D) mode. The other parameters are the same as in Fig. 1.

FIG. 7. Normalized growth rate (a) and real frequency (b) versus normalized perpendicular velocity shear v'_E for global (G) mode. The other parameters are the same as in Fig. 1.

FIG. 8. Normalized growth rate (a) and real frequency (b) versus normalized perpendicular velocity shear v'_E for double (D) mode. The other parameters are the same as in Fig. 1.

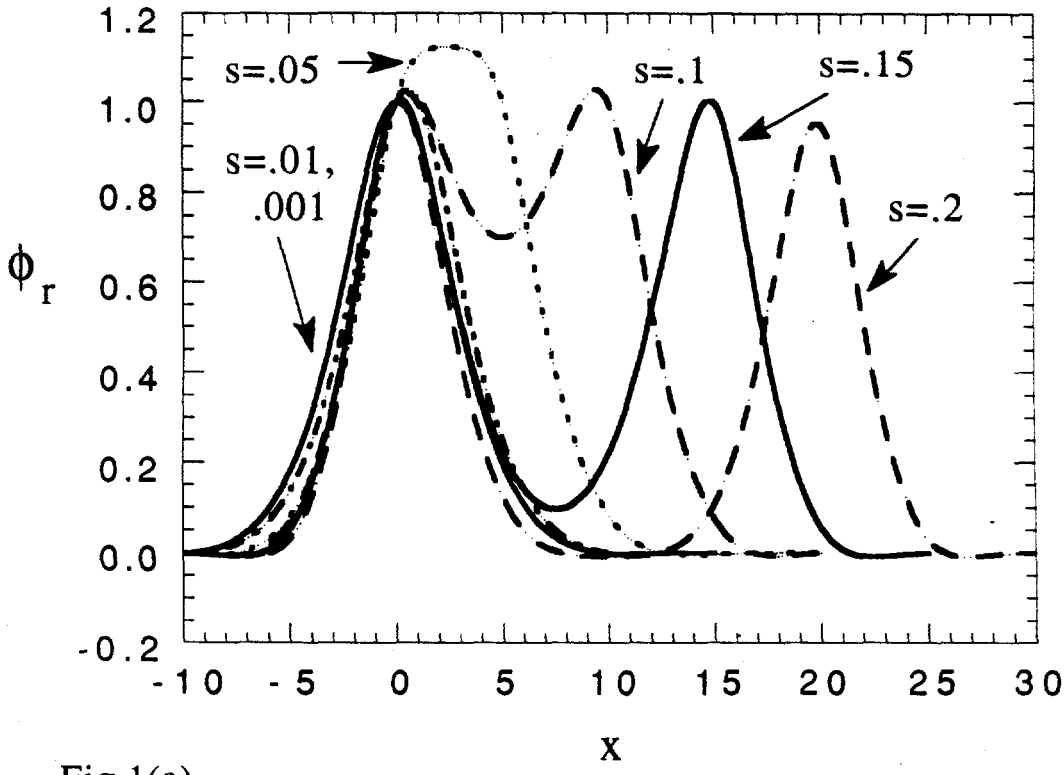
1.2
1.0
0.8
0.6
0.4
0.2
0.0
-0.2
ϕ_r
s=.05
s=.01,
.001
s=.1
s=.15
s=.2
-10
-5
0
5
10
15
20
25
30
x

Fig.1(a)

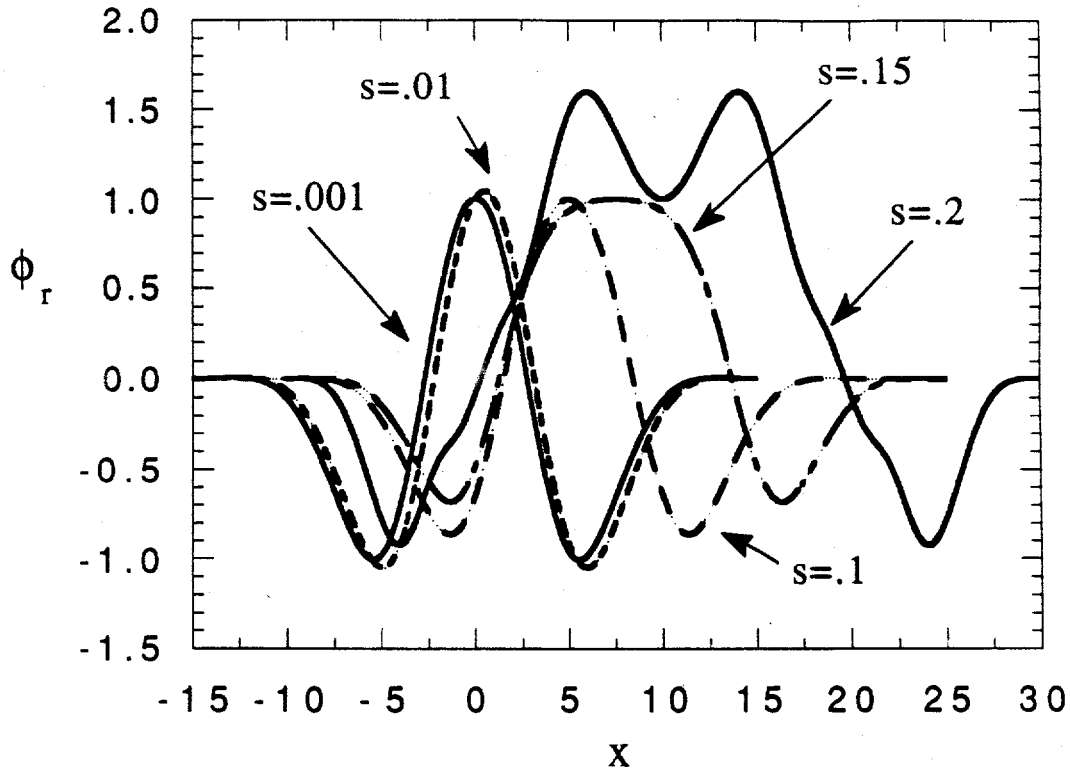
2.0
1.5
1.0
0.5
0.0
-0.5
-1.0
-1.5
ϕ_r
s=.01
s=.15
s=.001
s=.2
s=.1
-15 -10 -5 0 5 10 15 20 25 30
x

Fig.1(b)

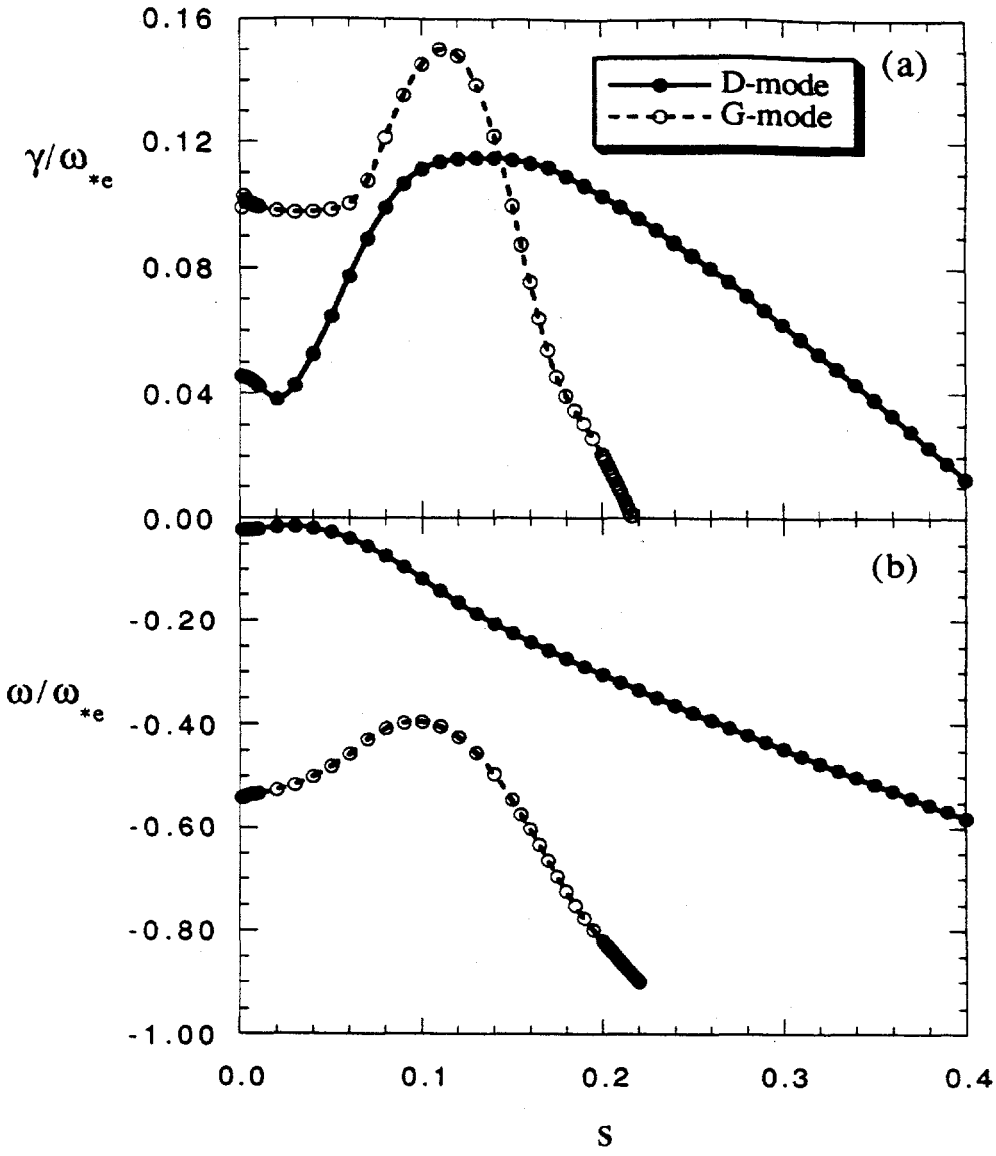
0.16
0.12
0.08
0.04
0.00
γ/ω*e
D-mode
G-mode
(a)
(b)
-0.20
-0.40
-0.60
-0.80
-1.00
ω/ω*e
0.0
0.1
0.2
0.3
0.4
s

Fig.2

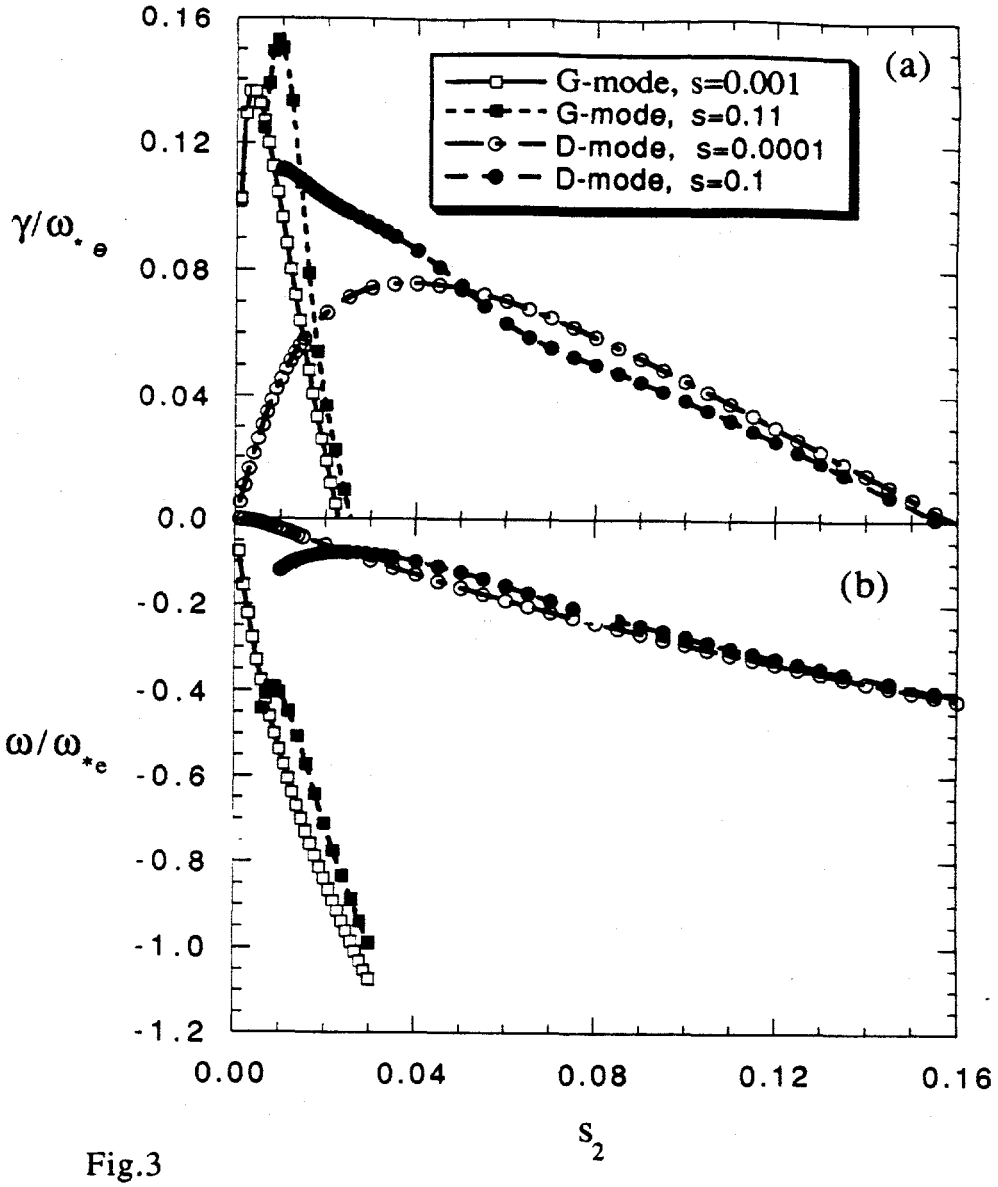
0.16
0.12
0.08
0.04
0.0
-0.2
-0.4
-0.6
-0.8
-1.0
-1.2
γ/ω*e
ω/ω*e
G-mode, s=0.001
G-mode, s=0.11
D-mode, s=0.0001
D-mode, s=0.1
(a)
(b)
0.00
0.04
0.08
0.12
0.16
s2

Fig.3

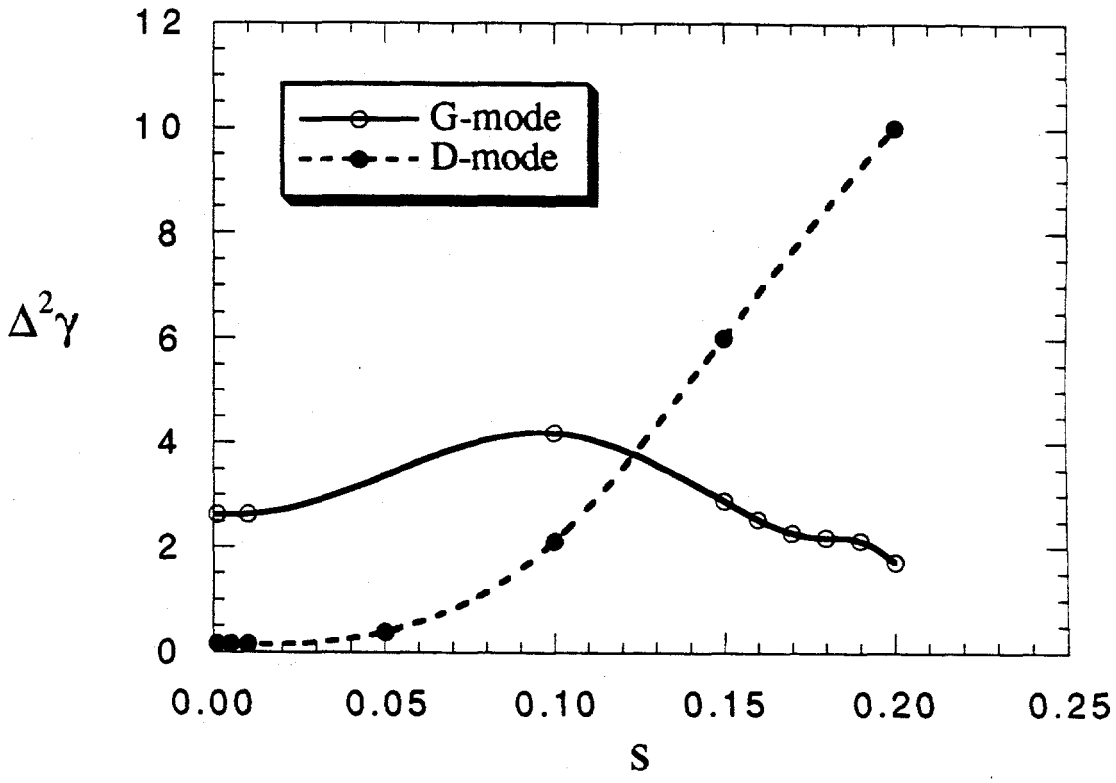

Fig.4

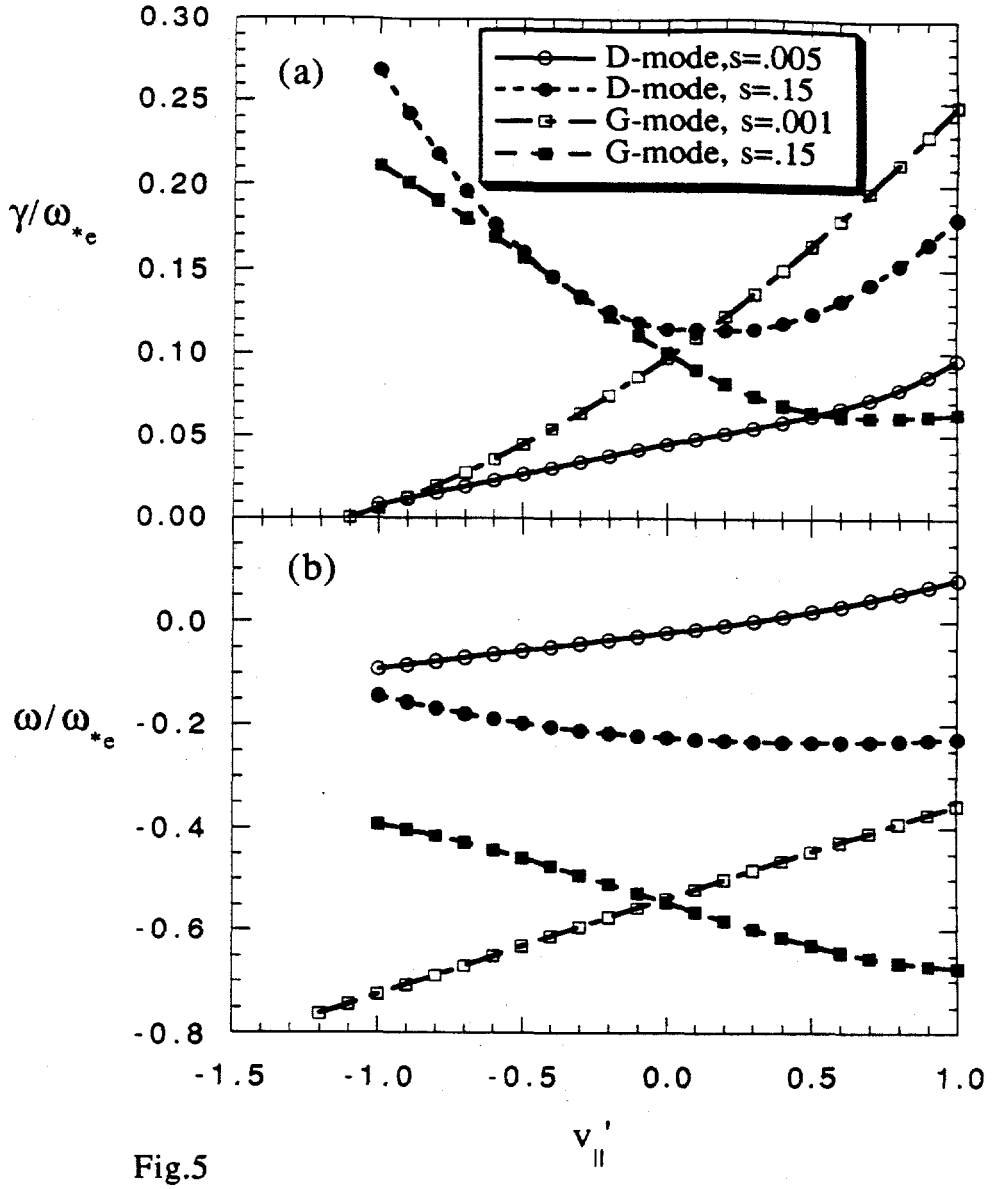
(a)
D-mode,s=.005
D-mode, s=.15
G-mode, s=.001
G-mode, s=.15
γ/ω*e
0.30
0.25
0.20
0.15
0.10
0.05
0.00
(b)
ω/ω*e
0.0
-0.2
-0.4
-0.6
-0.8
-1.5
-1.0
-0.5
0.0
0.5
1.0
v||'

Fig.5

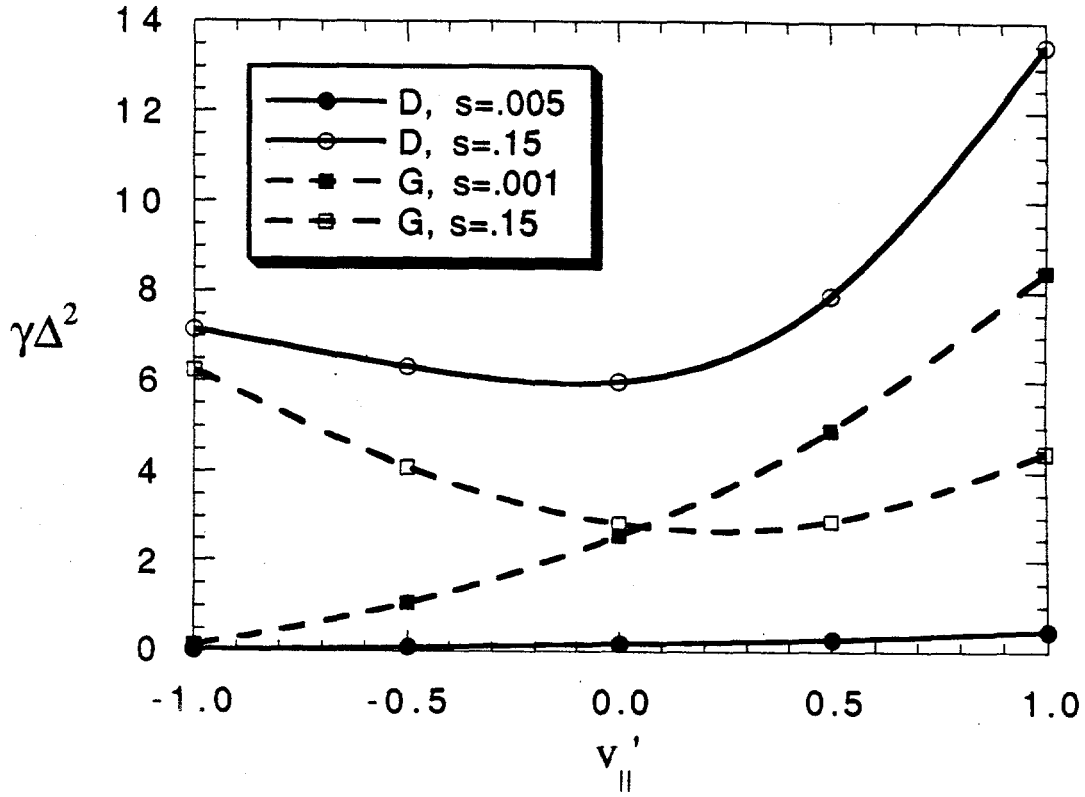
14
12
10
8
6
4
2
0
-1.0
-0.5
0.0
0.5
1.0
$\gamma\Delta^2$
$v_{\|}'$
D, s=.005
D, s=.15
G, s=.001
G, s=.15

Fig.6

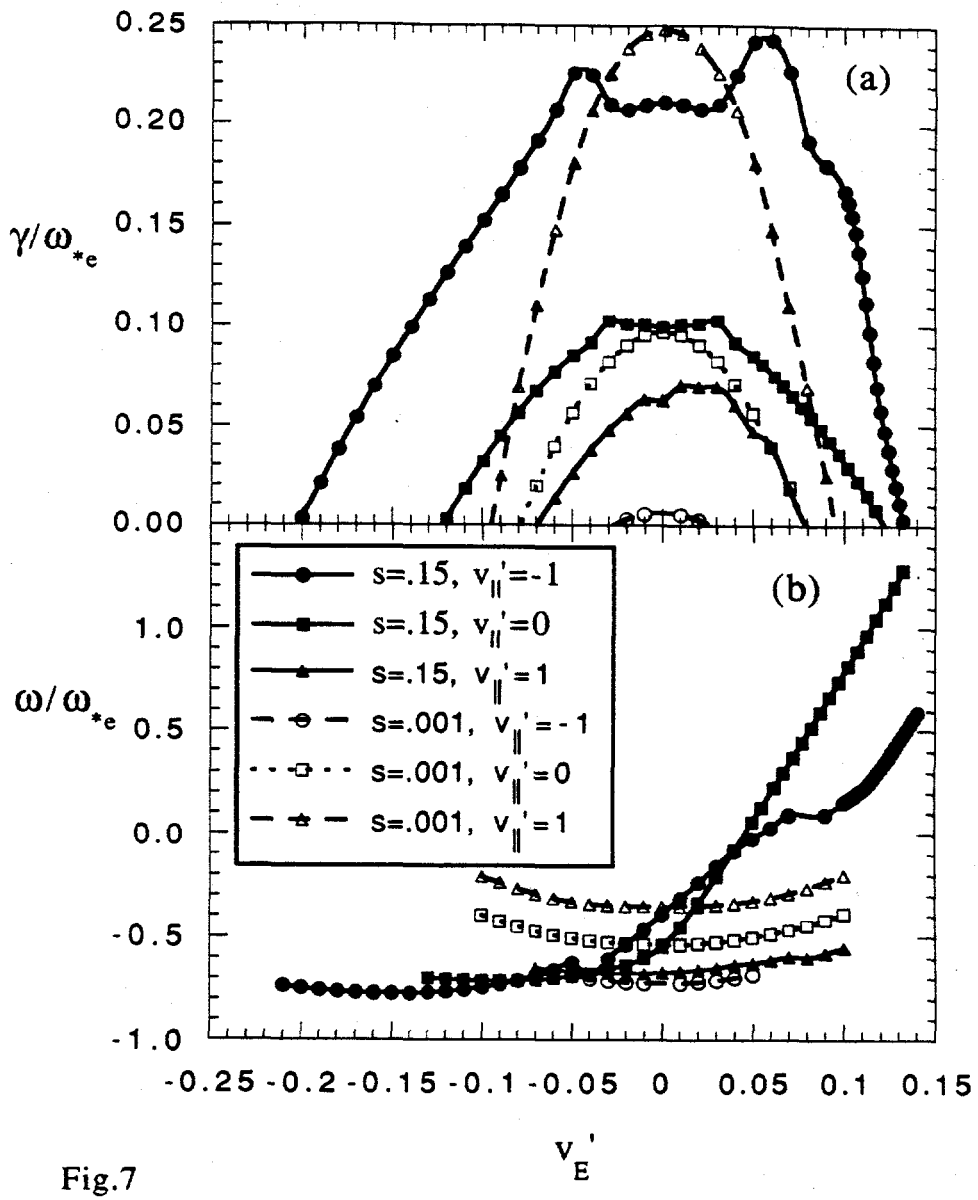
0.25
0.20
0.15
0.10
0.05
0.00
γ/ω*e
(a)
(b)
s=.15, v||'=-1
s=.15, v||'=0
s=.15, v||'=1
s=.001, v||'=-1
s=.001, v||'=0
s=.001, v||'=1
1.0
0.5
0.0
-0.5
-1.0
ω/ω*e
-0.25 -0.2 -0.15 -0.1 -0.05 0 0.05 0.1 0.15
v_E'

Fig.7

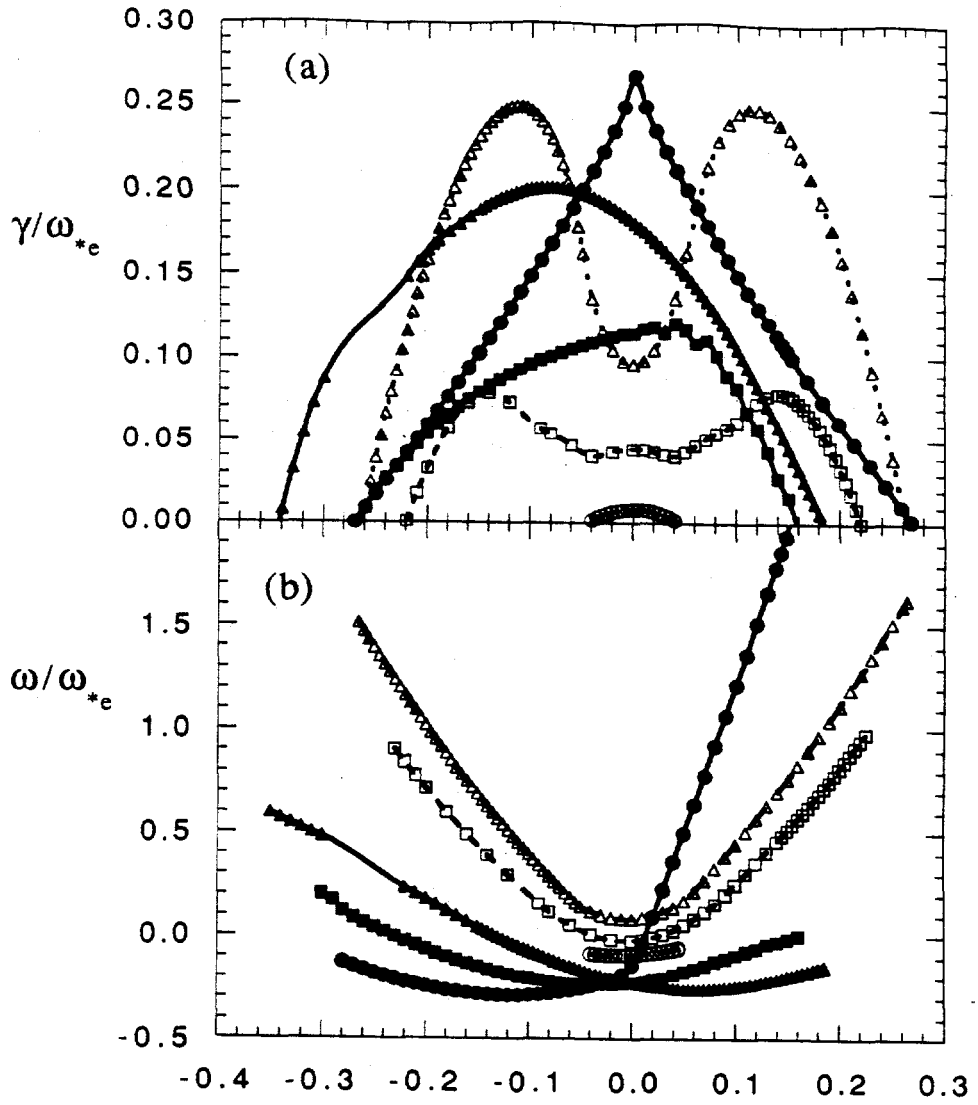
(a)
(b)
γ/ω_{*e}
ω/ω_{*e}
0.30
0.25
0.20
0.15
0.10
0.05
0.00
1.5
1.0
0.5
0.0
-0.5
-0.4
-0.3
-0.2
-0.1
0.0
0.1
0.2
0.3
v_E'

Fig.8